HD–THEP-99-53
M/C–TH-99/19
LPT-ORSAY-99-106

Observing the Odderon: Tensor Meson Photoproduction[1]

E. R. Berger[a], A. Donnachie[b], H. G. Dosch[c], O. Nachtmann[c]

[a] : LAPTH, Universite Paris-Sud, Batiment 211,
F-91405 Orsay Cedex, France

[b] : Department of Physics and Astronomy,
University of Manchester, Manchester M13 9PL, UK

[c] : Institut für Theoretische Physik der Universität Heidelberg,
Philosophenweg 16, D-69120 Heidelberg, Germany

Abstract

We calculate high-energy photoproduction of the tensor meson $f_2(1270)$ by odderon and photon exchange in the reaction $\gamma + \mathrm{p} \to f_2(1270) + \mathrm{X}$, where X is either the nucleon or the sum of the N(1520) and N(1535) baryon resonances. Odderon exchange dominates except at very small transverse momentum, and we find a cross section of about 20 nb at a centre-of-mass energy of 20 GeV. This result is compared with what is currently known experimentally about f_2 photoproduction. We conclude that odderon exchange is not ruled out by present data. On the contrary, an odderon-induced cross section of the above magnitude may help to explain a puzzling result observed by the E687 experiment.

[1] *email adresses*: berger@lyre.th.u-psud.fr, ad@a13.ph.man.ac.uk,
h.g.dosch@thphys.uni-heidelberg.de, o.nachtmann@thphys.uni-heidelberg.de

1 Introduction

In this paper we investigate the high-energy diffractive production of the tensor meson $f_2(1270)$ by real and virtual photons. Specifically we study $\gamma^{(*)}\mathrm{p} \to f_2\mathrm{X}$, where X is either the proton or the sum of the negative parity N(1520) and N(1535) resonances. For the latter two it is expected that the dominant exchange is the nonperturbative odderon [1], the $C = P = -1$ partner of the pomeron [2]. It has been shown [3] that the suppression of the odderon contribution in pp ($\bar{\mathrm{p}}\mathrm{p}$) scattering can be explained by diquark clustering in the proton, provided the diquark is sufficiently small ≤ 0.3 fm. This suppression does not operate if the nucleon dissociates into a negative parity state [4]. This paper is a continuation of the work presented in [4, 2] where the electroproduction of pseudoscalar mesons, in particular the reaction $\gamma^{(*)}\mathrm{p} \to \pi^0\mathrm{X}$ was studied. An explanation of the general philosophy of our approach and references to related work can be found there. A recent review about odderon physics is [5].

At sufficiently high energies only odderon and photon exchange contribute (Figure 1) to these reactions. Pomeron exchange does not contribute due to the positive charge parity of the f_2 (and of the pseudoscalars π^0 and η^0). Thus the energies available at HERA are an obvious attraction, and the cross sections, although small, are not unattainable. The two reactions, photoproduction of the tensor meson $f_2(1270)$ and photoproduction of the pseudoscalars π^0 or η^0 complement each other from the experimental viewpoint as the problems of detection and acceptance are very different. Given the rather small cross sections, if a signal is found in one reaction it is important to check that it is also there, at the appropriate level, in another.

In Section 2 we outline briefly the formalism for tensor meson production in γ^* p collisions. The next step is to construct a suitably normalised wave function for the f_2 which is done in Section 3. The odderon-exchange contribution is calculated in Section 4 and the photon exchange contribution in Section 5. The latter turns out to be about a factor of ten smaller than the odderon exchange. The results are discussed in Section 6 and compared with what is currently known experimentally about f_2 photoproduction. We conjecture that the current data can be interpreted as providing some evidence for odderon exchange although alternative and less exciting interpretations cannot be excluded. Appendices A and B contain respectively technical details of the calculation of the f_2 wave functions and of their overlap with the photon wave function.

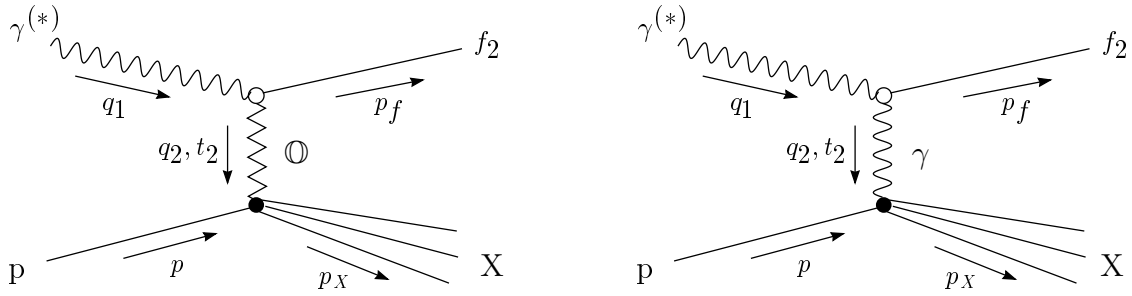

Figure 1: Feynman diagrams for f_2 production in the reaction $\gamma^{(*)}\mathrm{p} \to f_2\mathrm{X}$ at high energies with odderon (a) and photon (b) exchange.

2 Tensor meson production in the $\gamma^{(*)}\mathrm{p}$ reaction

We consider the production of the $J^{PC} = 2^{++}$ tensor meson $f_2(1270)$ in the reaction

$$\gamma^*(q_1) + \mathrm{p}(p) \to f_2(p_f) + \mathrm{X}(p_X). \tag{1}$$

Here we treat this reaction for photon virtualities $Q^2 \leq 5$ GeV^2 where $q_1^2 = -Q^2$ and in addition $q_2 = q_1 - p_f$, $t_2 = q_2^2$ and $W^2 = s_2 = (q_1 + p)^2$.

We start with the odderon exchange contribution of Figure 1a, which we calculate in the path integral approach [6, 7, 8]. It was shown in [2] that the final state X is dominated by the two negative parity isospin 1/2 resonances $N(1520)$ and $N(1535)$ with spin 3/2 and 1/2 respectively.

In the following we are interested in unpolarised cross sections and sum over these two final state resonances. In this case we can neglect the spin degree of freedom of the quark in the proton and the nucleonic excitations, which we treat as quark diquark-states with a scalar diquark [2]. In this way we can describe the odderon-proton interaction as the excitation of a spinless S-wave state (the proton) into a 2P state (either of the N^* states). The helicity amplitudes in the path integral approach are given by:

$$T(s_2, t_2)_{\lambda,\lambda_f,\lambda_\gamma} = 2is_2 \int d^2b\, e^{i\boldsymbol{q_{2T}}\boldsymbol{b}}\, \hat{J}_{\lambda,\lambda_f,\lambda_\gamma}(\boldsymbol{b}). \tag{2}$$

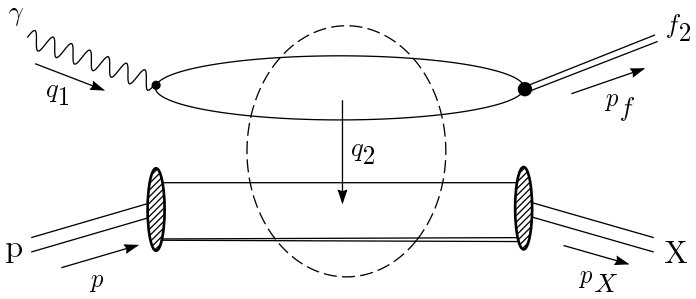

Figure 2: f_2 production in the reaction $\gamma^{(*)}\mathrm{p} \to f_2\mathrm{X}$. The dashed circle indicates the nonperturbative interaction (odderon exchange) of the colour dipoles.

Here λ, λ_f and λ_γ are respectively the 2P-state, the f_2 and the photon helicities. The profile function $\hat{J}$ is defined as

$$\hat{J}(\boldsymbol{b})_{\lambda,\lambda_f,\lambda_\gamma} = -\int \frac{d^2r_1}{4\pi}dz \int \frac{d^2r_2}{4\pi} \sum_{q,h,\bar{h}} \Psi^{*f}_{\lambda_f,\,qh_1h_2}(\boldsymbol{r}_1,z)\Psi^{\gamma}_{\lambda_\gamma,\,qh\bar{h}}(\boldsymbol{r}_1,z)$$
$$\times\, \Psi^{*\,2\mathrm{P}}_{\lambda}(\boldsymbol{r}_2)\Psi^{\mathrm{p}}(\boldsymbol{r}_2)\;\; \tilde{J}(\boldsymbol{b},\boldsymbol{r}_1,z,\boldsymbol{r}_2). \tag{3}$$

where z is the momentum fraction of the photon carried by the quark, q is a flavour index explained below (12) and $h, \bar{h}$ are respectively the quark and antiquark helicities. The physical picture underlying (2), (3) is shown schematically in Figure 2. The photon fluctuates into a $q\bar{q}$ pair, described by Ψ^γ. By soft colour interaction (odderon exchange), calculated from the functional integral of two lightlike Wegner-Wilson loops ($\tilde{J}$), the $q\bar{q}$ pair turns into the tensor meson f_2 and the proton (Ψ^{p}) is excited into a 2P wave ($\Psi^{2\mathrm{P}}$). An explicit expression for $\tilde{J}$ can be found in [4].

From (2) the cross section for $W^2 >> m_{\mathrm{p}}^2$ is given by:

$$d^2\sigma^{\mathbb{O}} = \frac{1}{8s_2}\frac{1}{(2\pi)^2}d^2k_T \sum_{\lambda}\sum_{\lambda_f}\sum_{\lambda_\gamma} |T_{\lambda,\lambda_f,\lambda_\gamma}|^2. \tag{4}$$

The wave functions occuring in (2) are light-cone wave functions [9]. We use the photon wave function for low virtualities as derived in [10] where it is argued that replacing the current quark mass in the expression for Ψ^γ calculated in light cone perturbation theory by a Q^2-dependent constituent quark mass $m(Q^2)$, with $m(0) \sim 0.21$ GeV, leads to a wave function which can also be used for photon virtualities $Q^2 \leq 1$ GeV^2. The nucleon wave functions Ψ^{p} and $\Psi^{2\mathrm{P}}$ can be found in [2].

The model as it stands gives no energy dependence of the cross sections, therefore all our numerical results refer to $W \approx 20$ GeV as the parameters are adapted to that energy. We expect the energy dependence of the soft odderon contribution to be similar to that of the soft pomeron as discussed in [2]. It should be recalled that the results for photoproduction of mesons by odderon exchange are particularly sensitive to the model parameters and the specific choice of the photon and meson wave function. As explained in [2] we estimate the overall uncertainty in our results to be about a factor of two.

3 The tensor meson wave function

To construct a light cone wave function for the tensor meson f_2, we use a similar procedure as developed in [11] to construct a wavefunction for the ρ.

We consider the f_2 to be a $q\bar{q}$ state consisting of on-shell quarks of mass $m(Q^2)$, with $m(0) \sim 0.21$ GeV, which moves with very large momentum in the 3-direction: $p_f = (p_f^0, \mathbf{0}_T, p_f^3)$ and $p_f^3 \to \infty$. To obtain the helicity structure of the wave function, we consider as interpolating operator the spin-two quark operator O,

$$O^{\mu\nu}(x) := \frac{1}{2}\bar{\psi}(x)\Big\{\gamma^{\{\mu} i\overleftrightarrow{\partial}^{\nu\}} - \tfrac{1}{2} i\overleftrightarrow{\not\partial}\, g^{\mu\nu}\Big\}\psi(x). \tag{5}$$

For clarity we explain our derivation of the helicity structure for only one flavour. The final result for the f_2 state will of course be written down with the appropriate flavour content. The vertex factor corresponding to (5) is

$$\begin{aligned} V^{\mu\nu}_{h\bar{h}}(p_q, p_{\bar{q}}) &:= \langle q(p_q, h),\, \bar{q}(p_{\bar{q}}, \bar{h})|O^{\mu\nu}(0)|0\rangle \\ &= \tfrac{1}{2}\bar{u}(p_q, h)\Big\{\gamma^{\{\mu} p_q^{\nu\}} - \gamma^{\{\mu} p_{\bar{q}}^{\nu\}} - m(Q^2) g^{\mu\nu}\Big\} v(p_{\bar{q}}, \bar{h}). \end{aligned} \tag{6}$$

The quark and the antiquark four-vectors p_q and $p_{\bar{q}}$ are parametrised by the relative transverse momentum $\boldsymbol{k}_T$ and the momentum fraction z of the f_2, carried by the quark. We have $p_q = (p_q^0, \boldsymbol{k}_T, zp_f^3)$, $p_{\bar{q}} = (p_{\bar{q}}^0, -\boldsymbol{k}_T, \bar{z}p_f^3)$ and $p_q^2 = p_{\bar{q}}^2 = m^2(Q^2)$ where $\bar{z} = (1-z)$.

Next we derive the polarisation tensors $e^{\mu\nu}(\lambda_f)$ for a massive spin-two particle. They can be constructed out of the polarisation vectors of a massive vector state

$$\begin{aligned} e^{\mu}_{\pm} &= (0, \mp 1, -i, 0)/\sqrt{2}, \\ e^{\mu}_{0} &= (p_f^3, 0, 0, p_f^0)/m_f, \end{aligned} \tag{7}$$

by use of the appropriate Clebsch-Gordan coefficients [13] and are given by

$$\begin{aligned} e^{\mu\nu}(\pm 2) &= e^{\mu}_{\pm} e^{\nu}_{\pm}, \\ e^{\mu\nu}(\pm 1) &= \sqrt{\tfrac{1}{2}}(e^{\mu}_{\pm} e^{\nu}_{0} + e^{\mu}_{0} e^{\nu}_{\pm}), \\ e^{\mu\nu}(0) &= \sqrt{\tfrac{1}{6}}(e^{\mu}_{+} e^{\nu}_{-} + e^{\mu}_{-} e^{\nu}_{+}) + \sqrt{\tfrac{2}{3}} e^{\mu}_{0} e^{\nu}_{0}. \end{aligned} \tag{8}$$

Here we do not use directly the polarisation tensors (8) but replace the longitudinal polarisation vector e_0 in (8) by $\tilde{e}_0 := e_0 - p_f/m_f$. This is justified neglecting terms of order $m(Q^2)/m_f \leq 15\%$. In any case this affects only the helicity states $0, \pm 1$ of the f_2 which will be shown below to give only a small contribution to the cross section.

Then we define the helicity structure $\tilde{\Psi}(\lambda_f)$, for a given f_2 helicity λ_f and quark and antiquark helicity h and $\bar{h}$ respectively, as the contraction of the vertex factor (6) with the corresponding polarisation tensor $e^{\mu\nu}(\lambda_f)$,

$$\tilde{\Psi}_{h\bar{h}}(\lambda_f) := \lim_{p_f^3 \to \infty} \frac{1}{p_f^3}\sqrt{p_q^3 p_{\bar{q}}^3}\, e_{\mu\nu}(\lambda_f) V^{\mu\nu}_{h\bar{h}}. \tag{9}$$

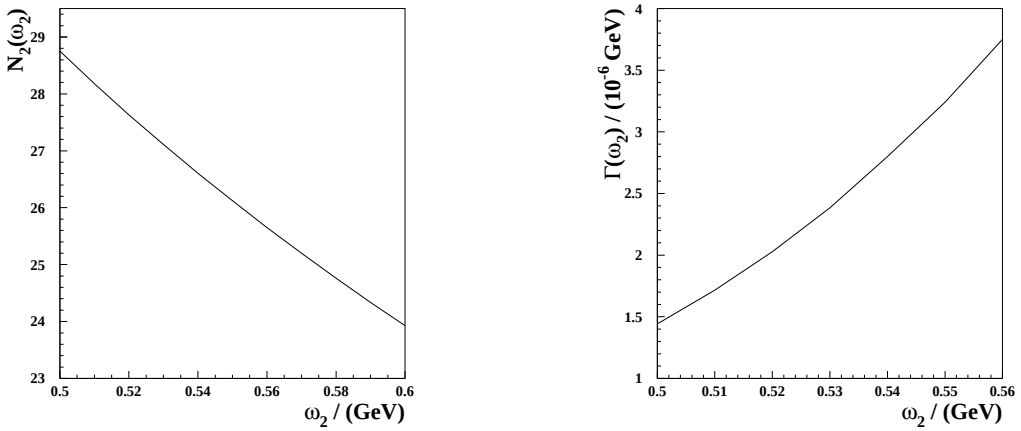

Figure 3: (a) The normalisation constant N_2 as a function of ω_2. (b) The partial decay width for a tensor meson f_2 with helicity 2 decaying into two photons (A.5) as a function of ω_2.

The f_2 helicity wave functions are then given by multiplying $\tilde{\Psi}_{h\bar{h}}(\lambda_f)$ with a Bauer-Stech-Wirbel (BSW) ansatz [12] for the transverse and longitudinal momentum distribution of the quarks in the f_2,

$$\tilde{f}_{\lambda_f}(k_T, z) = N_{\lambda_f}\,(z\bar{z})^{3/2}\, e^{-\frac{1}{2}m_f^2(z-1/2)^2/\omega_{\lambda_f}^2} \times \frac{2\pi}{\omega_{\lambda_f}^2 m_f} e^{-\frac{1}{2}k_T^2/\omega_{\lambda_f}^2}. \tag{10}$$

To define the helicity wave functions properly we first write down the f_2 state for helicity λ_f as follows:

$$\begin{aligned} |f_2(p_f, \lambda_f)\rangle := \int_0^1 dz \int_{-\infty}^{+\infty} \frac{d^2k_T}{16\pi^3} \frac{1}{\sqrt{z\bar{z}}} \sum_{qh\bar{h}} \tilde{\Psi}^f_{\lambda_f, qh\bar{h}} \\ \times \sqrt{\tfrac{1}{3}}\delta_{A\bar{A}} |q(p_q, h, A), \bar{q}(p_{\bar{q}}, \bar{h}, \bar{A})\rangle \end{aligned} \tag{11}$$

with the normalisation of the f_2 state chosen as

$$\langle f_2(p'_f, \lambda'_f | f_2(p_f, \lambda_f\rangle = 2p_f^0(2\pi)^3\delta^3(\boldsymbol{p}'_f - \boldsymbol{p}_f)\delta_{\lambda'_f\lambda_f}. \tag{12}$$

The index q in (11) is a flavour index, $q = u, d$, and $A, \bar{A}$ are colour indices. The wave functions $\tilde{\Psi}_{\lambda_f, qh\bar{h}}$ are the momentum space helicity wave functions of a quark-antiquark dipole with flavour q. They follow directly from (9),(10) and are given by

	$\lambda=2$	$\lambda=1$	$\lambda=0$
N_{λ_f}	27.11	38.78	47.33
ω_{λ_f}	0.53	0.60	0.36

Table 1: The numerical values for the normalisation constant N_{λ_f} and for the frequencies ω_{λ_f}.

$$
\begin{aligned}
\tilde{\Psi}^f_{\pm 2,qh\bar{h}} &= (\pm 2)\Big\{ m(Q^2)\,(k_1 \pm ik_2)\delta_{h\pm}\delta_{\bar{h}\pm} + \\
&\qquad (k_1 \pm ik_2)^2(z\delta_{h\pm}\delta_{\bar{h}\mp} - \bar{z}\delta_{h\mp}\delta_{\bar{h}\pm})\Big\} c_q\ \tilde{f}_2(k_T,z), \\
\tilde{\Psi}^f_{\pm 1,qh\bar{h}} &= (-1)\Big\{ m_f\, m(Q^2)\,(z-\bar{z})\delta_{h\pm}\delta_{\bar{h}\pm} \mp \\
&\qquad m_f\,(k_1 \pm ik_2)\Big((3z-4z^2)\delta_{h\pm}\delta_{\bar{h}\mp} + (3\bar{z}-4\bar{z}^2)\delta_{h\mp}\delta_{\bar{h}\pm}\Big)\Big\} c_q\ \tilde{f}_1(k_T,z), \\
\tilde{\Psi}^f_{0,qh\bar{h}} &= (-\sqrt{\tfrac{2}{3}})\Big\{ m(Q^2)\,\Big((k_1 - ik_2)\delta_{h+}\delta_{\bar{h}+} - (k_1+ik_2)\delta_{h-}\delta_{\bar{h}-}\Big) + \\
&\qquad (k_T^2 + 2z\bar{z}m_f^2)\Big((z-\bar{z})\delta_{h+}\delta_{\bar{h}-} - (\bar{z}-z)\delta_{h-}\delta_{\bar{h}+}\Big)\Big\} c_q\ \tilde{f}_0(k_T,z). \qquad (13)
\end{aligned}
$$

where $c_q = 1/\sqrt{2}$ for $q = u, d$. The constants N_{λ_f} are determined for each helicity by normalisation as a function of the frequencies ω_{λ_f}.

From (11),(12) it follows that the normalisation conditions of our helicity wave functions (13) are:

$$
\int_0^1 dz \int_{-\infty}^{+\infty} \frac{d^2k_T}{16\pi^3} \sum_{q,h,\bar{h}} |\tilde{\Psi}^f_{\lambda_f,qh\bar{h}}(\boldsymbol{k}_T,z)|^2 = 1. \qquad (14)
$$

In Figure 3a we show N_2 as a function of ω_2. To fix the frequencies ω_{λ_f} we need additional conditions. We use the partial decay width of the f_2 decaying into two photons, $\Gamma_{f_2\to\gamma\gamma}$, with the central value [13] being $\Gamma_{f_2\to\gamma\gamma} = 2.4$ keV. From rotational invariance it follows that the f_2 decays with the same decay width into two photons, independent of its helicity,

$$
\Gamma(f_2(\lambda_f) \to \gamma\gamma) = \Gamma_{f_2\to\gamma\gamma}. \qquad (15)
$$

In Appendix A we consider the f_2-decay for each helicity in the infinite momentum frame and calculate $\Gamma(f_2(\lambda_f) \to \gamma\gamma)$, defined in (A.3), as a function of the corresponding ω_{λ_f}. In Figure 3b we show our result, again for the case $\lambda_f = 2$. Then ω_2 is fixed by requiring (15). Using the value of ω_2 thus obtained we can read off from Figure 3a the corresponding normalisation factor N_2. For the other helicities we proceed in a similar way. The results for the normalisation constants and frequencies are listed in Table 1 ($\omega_{\lambda_f} = \omega_{-\lambda_f}, N_{\lambda_f} = N_{-\lambda_f}$). Now the momentum space wave functions (13) are fixed and it remains only to calculate the Fourier-transform in order to get the configuration-space wave functions needed in (2). This is done in Appendix B.

4 The odderon contribution

Now we come back to the helicity amplitudes. To calculate (2) we first have to consider the overlap functions between the photon and the f_2 wave functions. The explicit results are listed in (B.4), (B.5), (B.6) of Appendix B. As we can see there the dependence of all overlap functions on θ_1, the angle between $\boldsymbol{q}_{2_T}$ and $\boldsymbol{r}_1$, is given by a phase,

$$\sum_{f,h,\bar{h}} \Psi^{*f}_{\lambda_f,qh\bar{h}} \Psi^{\gamma}_{\lambda_\gamma,qh\bar{h}} = e^{i(\lambda_\gamma-\lambda_f)\theta_1} \Big[\sum_{f,h,\bar{h}} \Psi^{*f}_{\lambda_f,qh\bar{h}} \Psi^{\gamma}_{\lambda_\gamma,qh\bar{h}} \Big]_{\theta_1=0}. \tag{16}$$

Inserting (16) in (2) we can integrate over the angle θ_b, which is the angle between $\boldsymbol{b}_T$ and $\boldsymbol{q}_{2_T}$. We choose as new integration variables in (2) the relative angles between $\boldsymbol{b}_T$ and $\boldsymbol{r}_{1(2)}$, $\theta'_{1(2)} = \theta_{1(2)} - \theta_b$, where θ_2 is the angle between $\boldsymbol{q}_{2_T}$ and $\boldsymbol{r}_2$. In this way $\tilde{J}$ in (2) becomes independent of θ_b. By performing similar steps leading to (12) in [2] we get as the result for the helicity amplitudes:

$$\begin{aligned} T_{\lambda,\lambda_f,\lambda_\gamma} = {} & 2is_2 \int b\, db \int \frac{d^2r_1}{4\pi} dz \int \frac{d^2r_2}{4\pi} \\ & \times \Big[\sum_{q,h,\bar{h}} \Psi^{*f}_{\lambda_f,qh\bar{h}}(r_1,z) \Psi^{\gamma}_{\lambda_\gamma,qh\bar{h}}(r_1,z) \Big]_{\theta_1=0} \Psi^{*\,2\mathrm{P}}(r_2) \Psi^{\mathrm{P}}(r_2) \\ & \times e^{i((\lambda_\gamma-\lambda_f)\theta'_1+\lambda\theta'_2)} (i)^{(\lambda+\lambda_\gamma-\lambda_f)} 2\pi J_{(\lambda+\lambda_\gamma-\lambda_f)}(\sqrt{-t_2}b)\ \tilde{J}(\boldsymbol{b}_T, \boldsymbol{r}_1, z, \boldsymbol{r}_2). \end{aligned} \tag{17}$$

We note that for $\lambda = \lambda_f - \lambda_\gamma$ the forward amplitude does not vanish.

We first consider f_2 production by real photons. Using an argument similar to that in [2] we see that the amplitudes for $\lambda = 0$ vanish, so we have 20 helicity amplitudes contributing to the sum in (4). However, from (B.4) and (B.6) and noting that $J_{-n}(x) = (-1)^n J_n(x)$ it follows that

$$|T_{\lambda,\lambda_f,\lambda_\gamma}|^2 = |T_{-\lambda,-\lambda_f,-\lambda_\gamma}|^2 \tag{18}$$

and we are left with only 10 independent amplitudes. Of course (18) is a consequence of parity invariance. The result for the differential cross section is:

$$\frac{d\sigma^{\mathbb{O}}_t}{dt_2} = \frac{1}{16\pi} \frac{1}{s_2^2} \sum_{\lambda_f} \sum_{\lambda_\gamma} |T_{1,\lambda_f,\lambda_\gamma}|^2 \tag{19}$$

We show our result for the differential cross section in Figure 4. A first observation is that it looks quite similar to the differential cross section of π^0 production [2], but the normalisation is more than a factor of ten smaller. This can be understood by considering the flavour part of the π^0 and the f_2 wave functions. The π^0 has isospin one, so $\pi^0 \sim (u\bar{u} - d\bar{d})/\sqrt{2}$. This leads to a factor $\mathrm{e}/\sqrt{2}$ in the $\pi^0\gamma$-overlap as the flavour part of the photon wave function is $\gamma \sim (2u\bar{u} - d\bar{d})/3$. On the other hand in the case of the f_2 we have $f_2 \sim (u\bar{u} + d\bar{d})/\sqrt{2}$ and so we get $e/\sqrt{18}$ for the γf_2 overlap. This can simply be restated

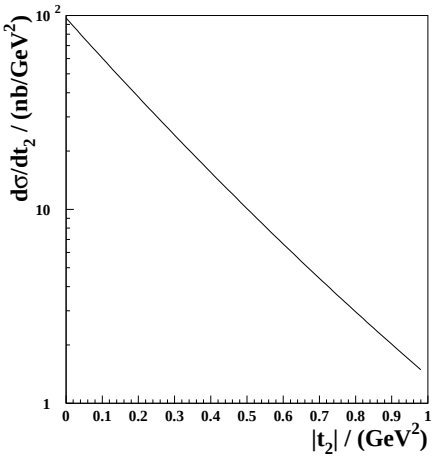

Figure 4: The differential cross section for $\gamma \mathrm{p} \to f_2 \mathrm{X}$. A fit to this curve is: $d\sigma_t^{\mathbb{O}}/dt_2 = a\ \exp(-b|t_2| + c|t_2|^2)$ where $a = 97$ nb/GeV$^2, b = 4.8$ GeV$^{-2}, c = 0.52$ GeV^{-4}.

that in the case of the π^0 the photon must be isovector while in the case of the f_2 the photon must be isoscalar. These factors enter quadratically into the cross section, so naively we expect the f_2 photoproduction cross section to be a factor of 9 smaller than that for the π^0.

Second, by computing the various helicity amplitudes we find that almost all of the cross section comes from the amplitudes $T_{1,2,1}$ and $T_{-1,-2,-1}$, where a helicity ± 1 photon is diffractively transformed into a helicity ± 2 tensor meson f_2. This means that the conservation of s-channel helicity is almost maximally violated at the particle level although it is fulfilled at the quark level. By integrating the differential distribution of Figure 4 we get for the total cross section:

$$\sigma^{\mathbb{O}}(\gamma\ \mathrm{p} \to f_2\ 2\mathrm{P}) = 21\ \mathrm{nb}. \tag{20}$$

Next we calculate the differential cross section for $Q^2 \neq 0$. In addition to (19) we define the longitudinal differential cross section as

$$\frac{d\sigma_l^{\mathbb{O}}}{dt_2} = \frac{1}{16\pi}\frac{1}{s_2^2}\sum_{\lambda}\sum_{\lambda_f}|T_{\lambda,\lambda_f,0}|^2. \tag{21}$$

In Figure 5a we compare the differential cross section for transversely and longitudinally polarised photons colliding with the proton for virtualities $Q^2 = 1, 4$ GeV^2. In addition we show in Figure 5b the integrated transverse and longitudinal cross section for $Q^2 \leq 5$ GeV^2, which is calculated by integrating (19), (21). With increasing photon virtuality the transverse cross section drops quite rapidly. From $Q^2 = 0$ to $Q^2 = 1$ GeV^2 the cross section decreases by more than a factor of five. At $Q^2 = 4$ GeV^2 the longitudinal cross section becomes comparable to the transverse one. However the decrease with increasing Q^2 is not so rapid as in the case of π^0 production by odderon exchange [4]. Due to the dependence of the constituent mass $m(Q^2)$ on Q^2 for $Q^2 \leq 1$ GeV^2, the cross section

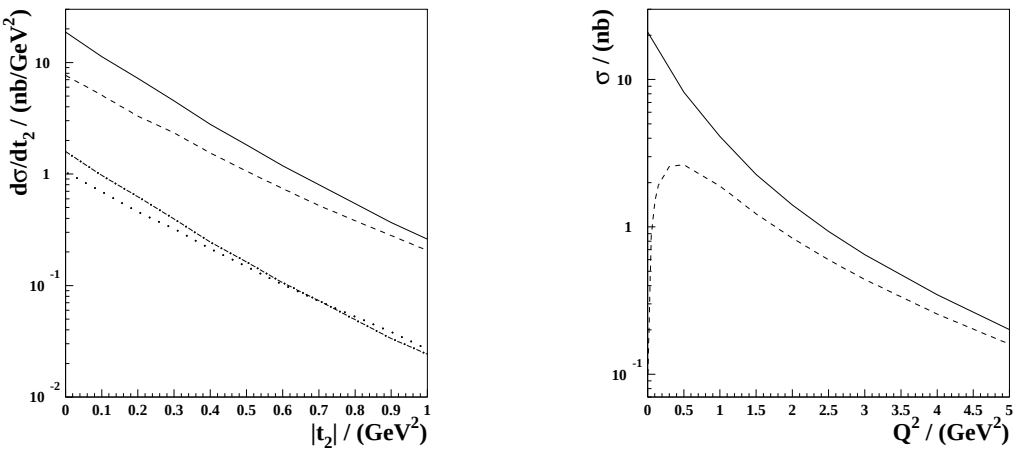

Figure 5: (a) The differential cross section for $\gamma^*\mathrm{p} \to f_2 X$ for $Q^2 = 1$ GeV^2 for transversely polarised photons (solid line) and longitudinally polarised photons (dashed line) and for $Q^2 = 4$ GeV^2 for transversely polarised photons (dashed dotted line) and for longitudinally polarised photons (dotted line). (b) The integrated cross section for transversely (solid line) and longitudinally (dashed line) polarised photons.

depends strongly on the weight of the terms in the overlap integrals which are proportional to $m(Q^2)$. For f_2 production this contribution is rather small (about 20% at $Q^2 = 0$). For π^0 production the terms in $m(Q^2)$ are significant, resulting in a steeper fall-off with increasing Q^2 as can be seen from Figure 8 of [4].

Finally we go from γ^*p to ep, restricting ourselves to small photon virtualities, $Q^2 < 0.01$ GeV^2 and applying the equivalent photon approximation (EPA) [14]. As the experimentally prefered observable we calculate the transverse momentum (k_T) distribution of the tensor meson f_2 with respect to the ep collision axis. Although k_T is formally defined as the transverse momentum of the f_2 with respect to the incoming photon we are allowed to identify it with the transverse momentum relative to the ep collision axis due to the restriction $Q^2 < 0.01$ GeV^2, at least for $k_T > 0.1$ GeV.

$$\frac{d\sigma_{\mathrm{ep}}^{\mathbb{O}}}{d|\boldsymbol{k}_T|} = c_{\mathrm{EPA}} \frac{1}{8\pi} \frac{1}{W^2} |\boldsymbol{k}_T| \sum_{\lambda_f} \sum_{\lambda_\gamma} |T_{1,\lambda_f,\lambda_\gamma}|^2. \tag{22}$$

Since the cross section (4) does not depend on the energy we just have to multiply it with a constant c_{EPA} given by the integral over the equivalent photon spectrum of the incoming electron. This constant depends on the phase space cuts applied. For the HERA "photoproduction" cuts (which in addition to $Q^2 < 0.01$ GeV^2 require $0.3 \leq y \leq 0.7$ where y is the energy fraction of the incoming electron carried by the photon in the proton rest

frame) $c_{\rm EPA} = 0.0136$ [2]. The result for the k_T distribution is shown as the solid line in Figure 6. This gives a total cross section for ep $\to$ e$f_2$2P by odderon exchange of ~ 285 pb.

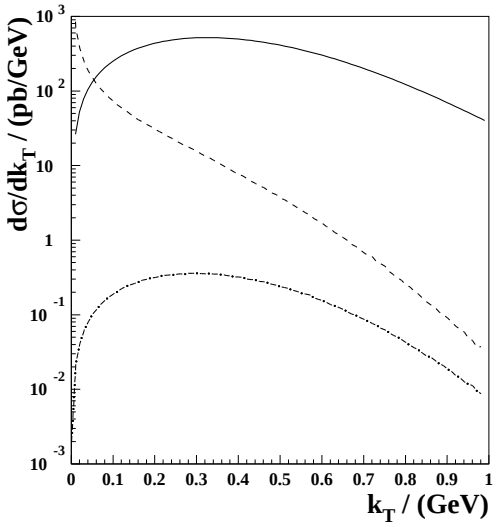

Figure 6: Transverse momentum distribution of the f_2 produced in ep collisions for odderon exchange (solid line), for photon exchange when the proton stays intact (dashed line) and for photon exchange, when the proton gets excited into the resonances N(1520), N(1535) (dashed dotted line).

5 The photon contribution

In this section we calculate the electromagnetic contribution Figure 1b. In contrast to diffractive f_2 production, in the electromagnetic case we get a contribution from "elastic" production, where the proton stays intact, as well as from "inelastic" production. In the following we calculate the two cases where either the proton stays intact or the proton gets exited into the resonances N(1520), N(1535).

We start with the "inelastic" case and calculate it in a similar way to the diffractive contribution. To do so we just have to do the replacement $\tilde{J} \to \tilde{J}^\gamma_q$ in (2),(3) where to lowest order in the electromagnetic coupling constant $\tilde{J}^\gamma_q$ describes one photon exchange between the $q\bar{q}$ pair from the photon and the quark-diquark pair of the proton,

$$\tilde{J}^\gamma_q = -ie^2 Q_q \Big\{ \frac{2}{3}\frac{K_0(\mu|\boldsymbol{b} + z\boldsymbol{r}_1 - \boldsymbol{r}_2/2|}{2\pi} - \frac{2}{3}\frac{K_0(\mu|\boldsymbol{b} - \bar{z}\boldsymbol{r}_1 - \boldsymbol{r}_2/2|}{2\pi} + \frac{1}{3}\frac{K_0(\mu|\boldsymbol{b} + z\boldsymbol{r}_1 + \boldsymbol{r}_2/2|}{2\pi} - \frac{1}{3}\frac{K_0(\mu|\boldsymbol{b} - \bar{z}\boldsymbol{r}_1 + \boldsymbol{r}_2/2|)}{2\pi} \Big\}. \qquad (23)$$

Here we have introduced a photon mass μ which will disappear in our final results. In addition Q_q is the quark charge, $Q_u = 2/3, Q_d = -1/3$.

We use (2),(3), replacing $\tilde{J}$ by $\tilde{J}^\gamma_q$. In this way each helicity amplitude consists of four terms proportional to the photon propagators in configuration space. Making a shift $\boldsymbol{b}$ in an appropriate way we can perform the $\boldsymbol{b}$ integrations in each of these contributions. In this way the photon propagator in momentum space enters. Then, finally we can also perform the θ_1, θ_2 integrations to get as result for the "inelastic" electromagnetic part of the helicity amplitudes:

$$
\begin{aligned}
T^\gamma_{\lambda,\lambda_f,\lambda_\gamma} = 2is_2 \int \frac{dr_1 r_1}{4\pi} dz \int \frac{dr_2 r_2}{4\pi} \Big[\sum_{q,h,\bar{h}} \Psi^{*f}_{\lambda_f,qh\bar{h}}(r_1,z) \Psi^\gamma_{\lambda_\gamma,qh\bar{h}}(r_1,z) \Big]_{\theta_1=0} \\
\times \Psi^{*\,2\mathrm{P}}(r_2) \Psi^{\mathrm{p}}(r_2) (\frac{5ie^2}{9}) \frac{1}{|t_2|} (2\pi)^2 \, i^{\lambda+\lambda_\gamma-\lambda_f} \\
\times \Big(J_{\lambda_\gamma-\lambda_f}(\sqrt{|t_2|} z r_1) - (-1)^{\lambda_\gamma-\lambda_f} J_{\lambda_\gamma-\lambda_f}(\sqrt{|t_2|}\bar{z} r_1) \Big) \\
\times \Big(2J_\lambda(\sqrt{|t_2|} r_2/2) + (-1)^\lambda J_\lambda(\sqrt{|t_2|} r_2/2) \Big). \qquad (24)
\end{aligned}
$$

The result for the "elastic" helicity amplitudes $T^\gamma_{\lambda_f,\lambda_\gamma}$ can be read off from (24) for $\lambda = 0$, replacing $\Psi^{2\mathrm{P}}$ by Ψ^{p}.

We concentrate directly on the ep reaction and apply the EPA, restricting ourselves again to HERA photoproduction cuts, and calculate the k_T spectrum (22) for the "elastic" and the "inelastic" case. The result is shown in Fig. 6. As in π^0 production photon exchange is dominated by odderon exchange for $k_T \geq 0.1$ GeV, but not by as much as in the former case. This can again be understood from consideration of the flavour parts. We couple two photons to the upper quark loop, which leads to a factor $(Q_q e)^2$. Now when summing over the flavours $q = u, d$, taking into account the flavour parts of the wave functions, we find in case of the π^0 a factor 1/9 and in case of the f_2 a factor 5/9. However, already for $k_T \geq 0.2$ the odderon contribution is more than a factor of ten larger than the electromagnetic contribution.

The integrated cross section gets most of its contributions from very small values of $|t_2|$, so the result is sensitive to the lower limit of $|t_2|$. Here we are specially interested in the value for the E687 experiment, where $\sqrt{s_2}$ is between 7 and 17 GeV. For the averaged value $\sqrt{s_2} = 12$ GeV we get a lower limit of about 0.0001 GeV^2. Using it we find for the ep reaction as integrated cross section for the electromagnetic contribution:

$$
\sigma^\gamma_{\mathrm{ep}}(\mathrm{e\,p} \to \mathrm{e}\, f_2\, \mathrm{p}) \approx 30\,\mathrm{pb} \qquad (25)
$$

which is about ten times smaller than the odderon cross section. As can be seen from Figure 6 the breakup by photon exchange is about a factor of 1000 smaller than the one induced by odderon exchange; interference terms between the odderon and the photon exchange are therefore to be expected at most on the 10 percent level.

6 Discussion

In this paper we have calculated the diffractive photo- and electroproduction of the f_2 at high energies. Our approach is based on functional integral techniques and the model of the stochastic vacuum to treat QCD in the nonperturbative region. We find a cross section of $\sim$ 20 nb for the odderon-exchange reaction $\gamma p \to f_2 X$ where the proton is required to break up. We estimate the overall uncertainty of our results to be about a factor of 2. In our model the elastic reaction $\gamma p \to f_2 p$ gets no contribution from odderon exchange in the strict quark-diquark limit for the proton structure. We also calculated the contributions from photon exchange instead of the odderon and found them to be small. We turn now to a discussion of the relevant experimental information.

In their high-statistics study of diffractively produced $\pi^+\pi^-$ states at high energy, $\langle\sqrt{s}\rangle \sim$ 12 GeV, the E687 Collaboration [15] has shown unambiguous evidence for the presence of the $f_2(1270)$. Its strength is between $\sim 0.1\%$ and $\sim 0.16\%$ of the ρ signal, depending on whether one or two ρ' states are included in the analysis. As an explanation of its observation the E687 collaboration suggested that as some particles, for example neutrals, could possibly be missed at such low relative yields the $f_2(1270)$ signal should be considerd as part of the background. However there are at least two other explanations. One is the mundane one of Regge exchange, specifically ρ and ω, as the energy of the experiment is not sufficiently high to exclude this possibility. The second is, of course, odderon exchange.

Cross sections are not quoted explicitly by E687 but production rates relative to the ρ are given. The experiment, which was designed primarily for charm photoproduction, used a 4cm long beryllium target and selected the $\pi^+\pi^-$ candidates from two-prong events with a veto on additional charged tracks and π^0's. Thus there is no information on the target particle and at some level events with N^* production must be present. We know that the diffractive ρ cross section at high energies is about 10 μb and the quasi-diffractive cross section with nucleon break-up is about 5 μb. These, together with the relative f_2 production rate, imply a cross section for the $f_2(1270)$ between $\sim$ 10 nb and $\sim$ 30 nb. That is, it is of the same order of magnitude as our calculated f_2 cross section from odderon exchange.

Let us look first at the alternative explanation, namely Regge exchange. In a diffractive $\pi^+\pi^-$ photoproduction experiment at $\sqrt{s} \sim 6$ GeV the SLAC Hybrid Photon Collaboration [16] saw no evidence for the $f_2(1270)$ in their $\pi^+\pi^-$ mass spectrum. The data in this experiment correspond to genuine elastic diffraction with no quasi-elastic events present in the final sample which was selected on the basis of a three-constraint kinematic fit. If the E687 f_2 signal were due to Regge exchange then, as we expect this cross section to vary approximately as s^{-1}, the f_2 signal at $\sqrt{s} \sim 6$ GeV would be $\sim$ 40 to $\sim$ 120 nb. This is comparable to the ρ' cross section of $\sim$ 130 nb and would have been visible in the experiment even at the lower limit. Of course, as explained earlier, we would not expect any odderon contribution to be seen in this experiment as nucleon break-up is specifically

excluded.

In a similar experiment the CERN Omega Photon Collaboration [17] at $\langle\sqrt{s}\rangle \sim 8.5$ GeV has also seen no evidence for the f_2 in their $\pi^+\pi^-$mass spectrum. The CERN experiment has lower statistics than the SLAC experiment, and the estimated Regge cross section is lower, lying between ~ 20 and ~ 60 nb. The upper end of this range can reasonably be ruled out but not the lower. The CERN experiment also differs from the SLAC experiment in that it cannot exclude some contamination from quasi-elastic events with nucleon break-up, so odderon exchange is allowed. Without a re-analysis of the data it is difficult to say categorically whether a cross section of 10 to 20 nb for the f_2 would be observable, although it does seem improbable.

Thus we can rather safely rule out Regge exchange as an explanation of the f_2 signal in the E687 experiment, but can retain the possibility of odderon exchange as an alternative to the "missing-particles" hypothesis. It may be purely coincidental that the experimental cross section for the f_2 is of the same order of magnitude as our calculation, but it is encouraging none the less. An additional and very relevant fact is that the t-dependence of the odderon term is significantly less strong than in diffractive ρ photoproduction, for example. This means that the f_2 cross section will appear to be relatively suppressed at small t, in conformity with the E687 data. Of course none of this is sufficient to claim that the odderon has been observed but it is sufficient to justify a new experimental study to confirm or deny this hypothesis.

The t-dependence of the cross sections for f_2 and π^0 are very similar, but the Q^2 dependence of the former is much less strong than for the latter. Thus although the f_2 cross section is a factor of about ten smaller than the π^0 cross section for production by real photons the difference is much less marked if a range of photon virtualities is considered and f_2 production is competitive.

The experiments H1 and ZEUS at HERA are ideally suited to clarify the situation since they have higher c.m. energy and can trigger on nucleon break-up. The challenge is then to observe a cross section of the order of 0.3 nb. for e p $\rightarrow$ ef_2X.

7 Acknowledgements

The authors would like to thank G. Kulzinger, P. V. Landshoff, P. Lebrun, K. Meier, H. J. Pirner, K. D. Rothe and M. Rueter for useful discussions and correspondence.

Supported in part by German Bundesministerium für Bildung und Forschung (BMBF), Contract Nr. 05 7HD 91 P(0); by the EU Programme "Training and Mobility of Researchers", Networks "Hadronic Physics with High Energy Electromagnetic Probes" (contract FMRX-CT96-0008); by "Quantum Chromodynamics and the Deep Structure of Elementary Particles" (contract FMRX-CT98-0194); by PPARC; by DAAD and by the EU programme "Human potential and mobility", Contract Nr. HPMF-CT-1999-00179.

A The decay of the f_2 into two photons

In this appendix we calculate the partial width of the decay $f_2 \to \gamma\gamma$ for the f_2 being in a definite helicity state, $\Gamma(f_2(\lambda_f) \to \gamma\gamma)$. We perform the calculation in the infinite momentum frame, where the three momentum of the f_2 is very large, $p_f^3 \to \infty$, and $\boldsymbol{p}_{f_T} = 0$.

The starting point of the following quark model calculation is the S-matrix element:

$$S_{fi} = \delta_{fi} + i(2\pi)^4\delta^4(\sum_f p_f - \sum_i p_i)T_{fi}, \tag{A.1}$$

$$T_{fi} = \langle\gamma(k_1,\lambda_1),\gamma(k_2,\lambda_2)|T|f_2(p_f,\lambda_f)\rangle := T(k_1,k_2;\lambda_1,\lambda_2;\lambda_f) =$$

$$\int \frac{d^2k_T}{(16\pi)^3}\,\frac{1}{\sqrt{z\bar{z}}}\sum_{q,h,\bar{h}} \tilde{\Psi}^f_{\lambda_f,qh\bar{h}}\sqrt{\tfrac{1}{3}}\delta_{A\bar{A}}\;\langle\gamma(k_1,\lambda_1),\gamma(k_2,\lambda_2)|T|q(p_q,h,A),\bar{q}(p_{\bar{q}},\bar{h},\bar{A})\rangle.$$

We calculate the partonic S-matrix element in (A.1) in lowest order perturbation theory.

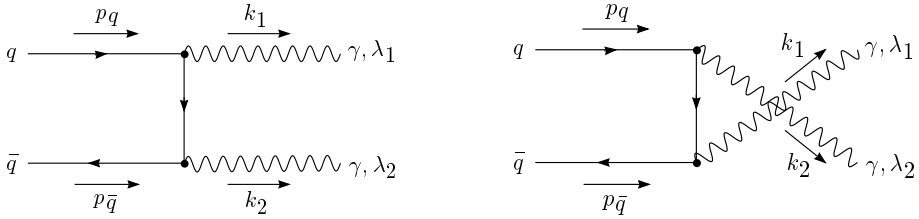

Figure 7: The Feynman diagrams for the partonic S-matrix element in (A.1)

The Feynman diagrams are shown in Figure 7. The corresponding analytic expression is:

$$\begin{aligned}\langle\gamma(k_1,\lambda_1),\gamma(k_2,\lambda_2)|T|q(p_q,h,A),\bar{q}(p_{\bar{q}},\bar{h},\bar{A})\rangle =\\ \times\,\delta_{A\bar{A}}\,Q_q^2e^2\,\bar{v}(p_{\bar{q}},\bar{h})\Big\{\,\not\epsilon\,(\lambda_2)\frac{(\not p_q - \not k_1 + m)}{(p_q-k_1)^2-m^2+i\epsilon}\not\epsilon\,(\lambda_1) +\\ \not\epsilon\,(\lambda_1)\frac{(\not p_q - \not k_2 + m)}{(p_q-k_2)^2-m^2+i\epsilon}\not\epsilon\,(\lambda_2)\;\Big\}u(p_q,h)\end{aligned} \tag{A.2}$$

Here Q_q is the quark charge. Combining (A.1) and (A.2) the decay rate of the f_2 with helicity λ_f is given by

$$\begin{aligned}\Gamma(f_2(\lambda_f)\to\gamma\gamma) = \int \frac{1}{2m_f}(2\pi)^4\delta^4(p_f-k_1-k_2)\\ \times\,\frac{1}{2}\frac{d^3k_1}{(2\pi)^3 2k_1^0}\frac{d^3k_2}{(2\pi)^3 2k_2^0}|T(k_1,k_2;\lambda_1,\lambda_2,\lambda_f)|^2\end{aligned} \tag{A.3}$$

where we have made the approximation $p_q + p_{\bar{q}} \approx p_f$. The factor $1/2$ reflects that the final state photons are indistingiushable.

Now, since we consider the decay in the infinite momentum frame of the f_2 it is useful to introduce light cone variables for the photon momenta k_1, k_2 when performing the phase space integral in (A.3),

$$\begin{aligned}\frac{d^3k_1}{(2\pi)^3 2k_1^0}\frac{d^3k_2}{(2\pi)^3 2k_2^0}\delta^4(p_f-k_1-k_2) = \\ \tfrac{1}{2}\prod_{i=1}^{2}\Big[dk_{i_+}dk_{i_-}d^2k_{i_T}\,\frac{1}{k_{i_+}}\delta(k_{i_-}-\frac{k_{i_T}^2}{k_{i_+}})\Big] \\ \delta(p_{f_+}-k_{1_+}-k_{2_+})\delta(p_{f_-}-k_{1_-}-k_{2_-})\delta^2(\boldsymbol{k}_{1_T}+\boldsymbol{k}_{2_T})\end{aligned} \tag{A.4}$$

From (A.4) one can see, that we are left with an integral over the transverse momentum of one photon, say $\boldsymbol{k}_{1_T} := \boldsymbol{q}_T$. Using (A.4) we finally get for the partial decay width:

$$\begin{aligned}\Gamma(f_2(\lambda_f)\to\gamma\gamma) = \frac{1}{8m_f}\frac{1}{(2\pi)^2}\sum_{j=+,-}\int d^2q_T \\ \times\frac{1}{m_f^2}\frac{1}{\sqrt{1-4q_T^2/m_f^2}}\sum_{\lambda_1,\lambda_2}|T_j(\boldsymbol{q}_T,\lambda_1,\lambda_2)|^2\end{aligned} \tag{A.5}$$

where we have to replace the plus, minus and transverse components of the photon momenta in (A.3) according to (A.4) by:

$$\begin{aligned}&\boldsymbol{k}_{1_T} = -\boldsymbol{k}_{2_T} = \boldsymbol{q}_T,\ k_{i_-} = \frac{q_T^2}{k_{i_+}}, \\ &k_{1_+} = \tfrac{1}{2}p_{f_+}(1\pm\sqrt{1-\frac{4q_T^2}{m_f^2}}) := q_\pm, \\ &k_{2_+} = \tfrac{1}{2}p_{f_+}(1\mp\sqrt{1-\frac{4q_T^2}{m_f^2}}) := q_\mp,\end{aligned} \tag{A.6}$$

Now we discuss (A.5) in more detail: First there occurs a sum over amplitudes $T_\pm$. For definite helicities of the photons they are defined as

$$\begin{aligned}T_+ &:= T(k_{1_+}\to q_+, k_{2_+}\to q_-), \\ T_- &:= T(k_{1_+}\to q_-, k_{2_+}\to q_+).\end{aligned} \tag{A.7}$$

where T are the amplitudes defined in (A.1). When translating them into the rest frame they correspond to the cases that either photon 1 (+) or photon 2 (−) has positive momentum in three direction. This becomes clear by looking at the expressions for k_{i_+} in (A.4). The (+) case corresponds to the upper signs and the (−) case to the lower ones.

Second, again by considering the decay in the rest frame it is clear, that no soft photon singularities can arise since the absolute value of the photon momenta is $m_f/2$. In principle a very soft photon can be produced by the boost into the infinite momentum frame when

the photons have only momentum in three direction. However, this special kinematical situation corresponds to $|\boldsymbol{q}_T| := q_T = 0$ in (A.5) and is supressed due to a factor q_T from the integration measure. Finally the sum over all photon polarisations does only depend on q_T and so the angle integration can be done trivially.

To calculate (A.5) we generate for every photon polarisation pair (λ_1, λ_2) explicit expressions for the matrix elements (A.1) using mathematica and calculate the integrals by numerical integration. After performing the sum over the photon polarisations in (A.5) we are left with a one dimensional integral over q_T, whose value depends on the frequency ω_{λ_f}. This integral $\Gamma(f_2(\lambda_f) \to \gamma\gamma)$ of (A.5) is plotted in Fig. 3 for the case $\lambda_f = 2$ as a function of ω_2.

B The Calculation of the $\gamma^* f_2$ overlap functions

In this appendix we calculate the Fourier transforms of the helicity wave functions (13) and the photon-tensor meson overlap functions. We start by defining the configuration space helicity wave functions:

$$\Psi^f_{\lambda_f,qh\bar{h}}(\boldsymbol{r}_1, z) := \int \frac{d^2k_T}{(2\pi)^2} e^{i\boldsymbol{k}_T\boldsymbol{r}_1} \tilde{\Psi}^f_{\lambda_f,qh\bar{h}}(\boldsymbol{k}_T, z) \tag{B.1}$$

The $\boldsymbol{k}_T$-dependence of the helicity structure of $\tilde{\Psi}$ can be expressed by spatial derivatives acting on the exponential in (B.1) and so, besides differentiating, it remains to calculate the Fourier transforms f_{λ_f} of the BSW functions (10) with the result

$$f_{\lambda_f}(r_1, z) = N_{\lambda_f}\,(z\bar{z})^{3/2}\, e^{-\frac{1}{2}m_f^2(z-1/2)^2/\omega^2_{\lambda_f}} \times \frac{1}{m_f} e^{-\frac{1}{2}r_1^2\,\omega^2_{\lambda_f}}. \tag{B.2}$$

In this way we find for the helicity wave functions of a $q\bar{q}$-dipole (13) in configuration space ($c_u = c_d = 1/\sqrt{2}$):

$$\begin{aligned}
\Psi^f_{\pm 2,qh\bar{h}} &= (\pm 2)\Big\{ im(Q^2) e^{\pm i\theta_1}\omega_2^2 r_1 \delta_{\pm\pm} \mp e^{\pm 2i\theta_1}\omega_2^4 r_1^2 (z\delta_{\pm\mp} - \bar{z}\delta_{\mp\pm})\Big\} c_q f_2,\\
\Psi^f_{\pm 1,qh\bar{h}} &= (-1)\Big\{ m_f m(Q^2)(z-\bar{z})\delta_{\pm\pm} \mp \\
&\qquad im_f e^{\pm i\theta_1}\omega_1^2 r_1((3z-4z^2)\delta_{\pm\mp} + (3\bar{z}-4\bar{z}^2)\delta_{\mp\pm})\Big\} c_q f_1,\\
\Psi^f_{0\,,qh\bar{h}} &= (-\sqrt{\tfrac{2}{3}})\Big\{ im(Q^2)\omega_0^2 r_1 (e^{-i\theta_1}\delta_{++} - e^{i\theta_1}\delta_{--}) + \\
&\qquad (2z\bar{z}m_f^2 - \omega_0^4 r_1^2 + 2\omega_0^2)((z-\bar{z})\delta_{+-} - (\bar{z}-z)\delta_{-+})\Big\} c_q f_0,
\end{aligned} \tag{B.3}$$

Next we use (B.3) together with the photon wave functions as given in (4)-(6) of [18] and calculate the $\gamma^* f_2$ overlap functions. With $\langle e\rangle = e/\sqrt{18}$ we find for transversly polarised

photons:

$$\sum_{q,h,\bar{h}} \Psi^{*f}_{+2,qh\bar{h}}\Psi^{\gamma}_{1,qh\bar{h}} = ie^{-i\theta_1}(-2)\sqrt{6}\langle e\rangle\Big\{m(Q^2)^2\omega_2^2 r_1\frac{K_0(\epsilon r_1)}{2\pi} + \omega_2^4 r_1^2(z^2+\bar{z}^2)\epsilon\frac{K_1(\epsilon r_1)}{2\pi}\Big\}f_2(r_1,z)$$

$$\sum_{q,h,\bar{h}} \Psi^{*f}_{-2,qh\bar{h}}\Psi^{\gamma}_{1,qh\bar{h}} = ie^{3i\theta_1}(2)\sqrt{6}\langle e\rangle\Big\{\omega_2^4 r_1^2(2z\bar{z})\epsilon\frac{K_1(\epsilon r_1)}{2\pi}\Big\}f_2(r_1,z)$$

$$\sum_{q,h,\bar{h}} \Psi^{*f}_{+1,qh\bar{h}}\Psi^{\gamma}_{1,qh\bar{h}} = (-1)\sqrt{6}\langle e\rangle\Big\{m_f m(Q^2)^2(z-\bar{z})\frac{K_0(\epsilon r_1)}{2\pi} + m_f\omega_1^2 r_1(z-\bar{z})(1-4z\bar{z})\epsilon\frac{K_1(\epsilon r_1)}{2\pi}\Big\}f_1(r_1,z)$$

$$\sum_{q,h,\bar{h}} \Psi^{*f}_{-1,qh\bar{h}}\Psi^{\gamma}_{1,qh\bar{h}} = e^{2i\theta_1}\sqrt{6}\langle e\rangle\Big\{m_f\omega_1^2 r_1(\bar{z}-z)(4z\bar{z})\epsilon\frac{K_1(\epsilon r_1)}{2\pi}\Big\}f_1(r_1,z)$$

$$\sum_{q,h,\bar{h}} \Psi^{*f}_{0,qh\bar{h}}\Psi^{\gamma}_{1,qh\bar{h}} = ie^{i\theta_1}2\langle e\rangle\Big\{m(Q^2)^2\omega_0^2 r_1\frac{K_0(\epsilon r_1)}{2\pi} - (2z\bar{z}m_f^2 - \omega_0^4 r_1^2 + 2\omega_0^2)(z-\bar{z})^2\epsilon\frac{K_1(\epsilon r_1)}{2\pi}\Big\}f_0(r_1,z) \qquad \text{(B.4)}$$

The $\gamma^* f_2$ overlap functions for longitudinally polarised photons are:

$$\sum_{q,h,\bar{h}} \Psi^{*f}_{+2,qh\bar{h}}\Psi^{\gamma}_{0,qh\bar{h}} = Qe^{-2i\theta_1}2\sqrt{3}\langle e\rangle\Big\{\omega_2^4 r_1^2(z-\bar{z})(2z\bar{z})\frac{K_0(\epsilon r_1)}{2\pi}\Big\}f_2(r_1,z),$$

$$\sum_{q,h,\bar{h}} \Psi^{*f}_{+1,qh\bar{h}}\Psi^{\gamma}_{0,qh\bar{h}} = Qie^{-i\theta_1}\sqrt{3}\langle e\rangle\Big\{m_f\omega_1^2 r_1(2z\bar{z}) \times((3z-4z^2)+(3\bar{z}-4\bar{z}^2))\frac{K_0(\epsilon r_1)}{2\pi}\Big\}f_1(r_1,z),$$

$$\sum_{q,h,\bar{h}} \Psi^{*f}_{0,qh\bar{h}}\Psi^{\gamma}_{0,qh\bar{h}} = Q\sqrt{2}\langle e\rangle\Big\{(2z\bar{z}m_f^2 - \omega_0^2 r_1^2 + 2\omega_0^2) \times(2z\bar{z})2(z-\bar{z})\frac{K_0(\epsilon r_1)}{2\pi}\Big\}f_0(r_1,z), \qquad \text{(B.5)}$$

Finally the remaining overlap functions are simply related to the overlap functions (B.4), (B.5) by:

$$\sum_{q,h,\bar{h}} \Psi^{*f}_{+\lambda_f,qh\bar{h}}\Psi^{\gamma}_{+\lambda_\gamma,qh\bar{h}} = \Big(\sum_{q,h,\bar{h}} \Psi^{*f}_{-\lambda_f,qh\bar{h}}\Psi^{\gamma}_{-\lambda_\gamma,qh\bar{h}}\Big)^*, \qquad \text{(B.6)}$$

References

[1] L Lukaszuk and B Nicolescu: Nuov. Cim. Lett. **8**, 405 (1973);
D Joynson, E Leader, C Lopez and B Nicolescu: Nuov. Cim. **A30**, 345 (1975)

[2] E R Berger, A Donnachie, H G Dosch, W Kilian, O Nachtmann and M Rueter: Eur. Phys. J. **C9**, 491 (1999)

[3] M Rueter and H G Dosch: Phys. Lett. **B380**, 177 (1996)

[4] M Rueter, H G Dosch and O Nachtmann: Phys. Rev. **D59**, 014018 (1999)

[5] B Nicolescu: report hep-ph/9911334

[6] O Nachtmann: Ann. Phys. **209**, 436 (1991)

[7] H G Dosch, E Ferreira and A Krämer: Phys. Rev. **D50**, 1992 (1994)

[8] O Nachtmann: in *Perturbative and Nonperturbative Aspects of Quantum Field Theory*, edited by H Latal and W Schweiger (Springer Verlag, Berlin, Heidelberg 1997)

[9] J D Bjorken, J B Kogut and D E Soper: Phys. Rev. **D3**, 1382 (1971);
G P Lepage and S J Brodsky: Phys. Rev. **D22**, 2157 (1980);
G P Lepage: in *Proceedings of the Banff Summer Institut, Particles and Fields 2*, Banff (Canada 1982)

[10] H G Dosch, T Gousset and H J Pirner: Phys. Rev. **D57**, 1666 (1998)

[11] H G Dosch, T Gousset, G Kulzinger and H J Pirner: Phys. Rev. **D55**, 2602 (1997)

[12] M Wirbel, B Stech and M. Bauer: Z. Phys. **C29**, 637 (1985)

[13] R M Barnett et al (Particle Data Group): Eur. Phys. J. **C3**, 1 (1998)

[14] V M Budnev, I F Ginzburg, G V Meledin and V G Serbo: Phys. Rep. **15**, 181 (1975)

[15] P Lebrun: *Proceedings of HADRON'97* p.504, edited by S-U Chung and H J Willetski (AIP Conference Proceedings 432, 1997);
E687: private communication

[16] K. Abe et al: Phys.Rev.Lett. **53** (1984) 751

[17] D Aston et al: Phys.Lett. **92B** (1980) 215

[18] G Kulzinger, H G Dosch and H J Pirner: Eur. Phys. J. **C7**, 73 (1999)